In the above protocols the reaction mixture was contaminated by small amounts of starting materials, but the high yields enabled facile isolation of the pure product esters by column chromatography.[6] There is no problem so long as the isolation of the esters is solely targeted. However, this is not the case in practical processes wherein the remaining reactants need to be recovered. The 1:1 stoichiometry is truly effective only if the 100% conversion is reached because otherwise the two components (recovered carboxylic acid and alcohol) should be separated from the product mixture, which is a less favorable situation than the reaction employing one of the reactants in excess. In this case, the recovery of only one reactant is necessitated on account of the more facile feasibility of the 100% conversion. As such, the 100% yield with equimolar amounts of the reactants which demands no purification step still remains a challenge. The levels of conversion and yield attained in the above studies are not satisfactory in such a strict sense. Nevertheless, these protocols have no doubt made a big step forward along this line and, accordingly, these achievements are expected to pave the way to the ultimate goal.

[1] T. W. Greene, P. G. Wuts, *Protective Groups in Organic Synthesis*, 3rd ed., Wiley, New York, **1999**, p. 149 and p. 373.
[2] B. M. Trost, *Science* **1991**, *254*, 1471; B. M. Trost, *Angew. Chem.* **1995**, *107*, 285–307; *Angew. Chem. Int. Ed. Engl.* **1995**, *34*, 259–281..
[3] For recent representative examples, see G. A. Olah, T. Keumi, D. Meidar, *Synthesis* **1978**, 929; A. K. Kumar, T. K. Chattopadhyay, *Tetrahedron Lett.* **1987**, *28*, 3713; J. Otera, N. Dan-oh, H. Nozaki, *J. Org. Chem.* **1991**, *56*, 5307; B. Das, B. Venkataiah, P. Madhusudhan, *Synlett* **2000**, 59; A. S.-Y. Lee, H.-C. Yang, F.-Y. Su, *Tetrahedron Lett.* **2001**, *42*, 301.
[4] K. Ishihara, S. Ohara, H. Yamamoto, *Science* **2000**, *290*, 1140.
[5] K. Wakasugi, T. Misaki, K. Yamada, Y. Tanabe, *Tetrahedron Lett.* **2000**, *41*, 5249.
[6] Professor Hisashi Yamamoto, private communication; the isolation method is not described in ref. [4].

Recent Advances in High-Resolution Solid-State NMR Spectroscopy**

Harald Schwalbe* and Anthony Bielecki

It has long been known that NMR spectroscopy can yield precise information about the structure and dynamics of large biological molecules. The vast majority of NMR studies have been carried out on liquid solution samples owing to the good resolution, namely narrower peaks, as compared to solid samples. Even so, it is often necessary to study the solid state for insoluble biopolymers, such as aggregates or amyloids. There are also significant classes of materials whose properties lie between the solid and liquid states: Membranes and membrane-bound proteins are not strictly solid and may be more accurately described as liquid crystals, since they have a high degree of molecular alignment. Other examples would be extremely viscous liquids or gels, where the molecular mobility is slow or limited. For all of these systems, solid-state NMR investigations can be particularly useful. The question then is not whether to study the liquid or solid form, but how one can get the best information from solid-state NMR methods.

[*] Prof. Dr. H. Schwalbe, Dr. A. Bielecki
Department of Chemistry
and MIT/Harvard Center for Magnetic Resonance
at the Francis Bitter Magnet Laboratory
Massachusetts Institute of Technology
77 Massachusetts Avenue, Cambridge, MA 02139 (USA)
Fax: (+1) 617-253-5405
E-mail: schwalbe@mit.edu

[**] We thank the Massachusetts Institute for Technology, the Karl Winnacker Foundation, and the NIH under the NCRR program (RR00995) for financial support. We thank Elke Duchardt for helping us prepare the figures.

The difficulties of solid-state NMR are due to large anisotropic interactions, namely the through-space dipole–dipole coupling, more often called the dipolar coupling, and the orientational dependence of the chemical shift, called the chemical shift anisotropy (CSA). (Some nuclei possess an electric quadrupole moment, which creates yet another anisotropic interaction, but that will not be discussed further in this article.) Rapid molecular motion in the liquid state removes anisotropic interactions, except for their effects on relaxation. However, in solids these interactions are present at their full strength and they must be dealt with appropriately. There are different experimental approaches in solid-state NMR spectroscopy, depicted in Figure 1, which either circumvent or utilize these anisotropic interactions in order to investigate structures of biological systems.

MAS Solid-State NMR

One approach is to use magic-angle spinning (MAS) in combination with high-power radio-frequency decoupling to remove the chemical shift anisotropy and the dipolar couplings (Figure 1a). MAS spectra of solids often exhibit sharp resonances at frequencies determined solely by the isotropic chemical shift. In this respect, they resemble NMR spectra of liquids, and the information content is at least qualitatively similar. For example, in multidimensional MAS spectra, chemical-shift correlations are measured, and these yield information about connectivity and proximity, just as in multidimensional NMR of solutions. In the past, MAS solid-

  1433-7851/01/4011-2045 $ 17.50+.50/0

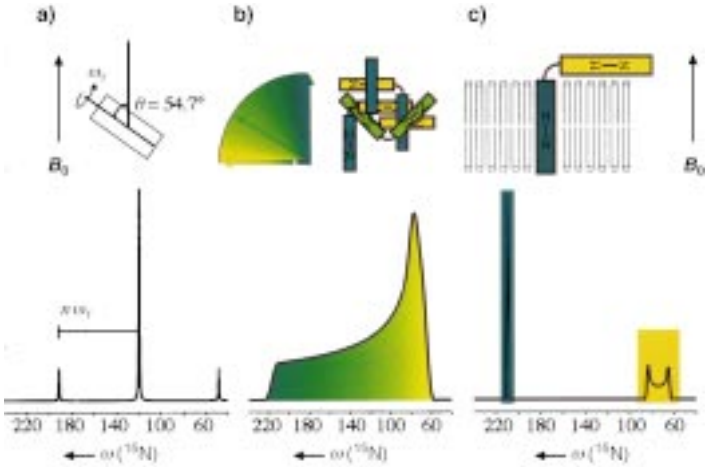

Figure 1. Three methods in solid-state NMR. Above are the experimental approaches, below are the matching ^{15}N NMR spectra. a) In magic-angle spinning (MAS) NMR, the sample is rotated with a rotation speed ω_r around an axis with an angle 54.7° ($=\theta \approx \cos^{-1}\sqrt{1/3}$) relative to the magnetic field $\boldsymbol{B}_0$. This leads to an averaging of anisotropic interactions such as dipolar couplings and chemical shift anisotropy. Additional peaks arise from spinning sidebands at multiples of the rotor frequency $n\omega_r$. b) In solid-state NMR of orientationally disordered samples, a broad frequency distribution is observed that reflects the orientational dependence of the chemical shift, the CSA. c) In solid-state NMR of samples oriented in lipid bilayers, the observed chemical shift depends on the orientation of a specific site relative to the bilayer normal. Experimentally, the bilayer normal axis is mechanically oriented parallel to the $\boldsymbol{B}_0$ field.

state NMR experiments on biological systems have often been performed with samples that were labeled at specific sites with NMR-active isotopes, such as ^{13}C or ^{15}N. These studies have focused on the investigation of one specific structural question at a time and yielded, for example, selected internuclear distances with very high precision. However, selective-labeling schemes lack generality. Therefore, a number of recent reports of nearly complete resonance assignments in uniformly ^{13}C,^{15}N-labeled proteins by MAS solid-state NMR have generated considerable excitement.

The groups of McDermott, Zilm, and Montelione[1] have studied BPTI, a 6.5 kDa protein with 58 residues, and the groups of Baldus, de Groot, and Oschkinat[2] have reported the ^{13}C,^{15}N resonance assignments of an SH3 domain of 62 residues. Part of the success in both reports stems from the optimized sample preparation conditions that could be found, which yielded narrow line widths in the MAS solid-state spectra. For overexpressed BPTI, microcrystallites were obtained by dialysis methods. For the SH3 domain, different sample preparation methods were compared: a) lyophilization from an aqueous low-salt buffer, b) lyophilization retaining hydration water, c) lyophilization from a solution containing PEG-8000 and sucrose, and d) precipitation from a concentrated $(NH_4)_2SO_4$ solution.[3] The differences in the spectral quality depending on the sample preparation are impressive: The observed line width could be reduced from 190 to 70 Hz for the precipitated SH3 (condition d). Pauli et al.[2] then showed that, on having such systems in hand, almost complete resonance assignments in uniformly ^{13}C,^{15}N-labeled proteins can be achieved by solid-state NMR spectroscopy. A representative spectrum, correlating nitrogen amide backbone nuclei with side chain carbon nuclei from their report is shown in Figure 2.

The report of two uniformly labeled protein systems amenable to MAS solid-state spectroscopy allows optimization of assignment procedures under realistic conditions even for larger protein systems in the solid state. Based on previous methodological developments,[4] Pauli et al. have used three different experimental schemes for solid-state spectra: The first correlation experiments, NCO and NCA, established connectivity between the amide nitrogen and the directly bound C′ and C_α atoms, respectively. Such selective coherence transfers can be achieved in band-selective experiments.[5] In the next two experiments, one additional transfer step is added to transfer coherence from the C′ and C_α atoms into the inter- and intraresidual carbon network, respectively. Depending on the contact time used in these experiments, coherence transfer is predominantly observed to directly bound carbon or to remote carbon atoms.

McDermott et al.[1] commented that the resonance assignments in the solid state show that the isotropic chemical shifts in the solid state are similar to those in the liquid state for the majority of the observed cross peaks. This makes it feasible to transfer chemical shift assignments obtained in solution to the solid-state spectra. Such resonance assignment transfer is an attractive tool, if chemical shifts and their perturbation, such as in the presence of a ligand interacting with a target protein in a lipid environment, are to be compared. At the same time, methods are being developed to measure internuclear $^{13}C-^{13}C$ and $^{13}C-^{15}N$ distances[6] as well as torsion angle restraints[7] in uniformly labeled proteins, which holds promise for the structure determination of proteins in their solid state.

The investigations also underline the importance of high magnetic-field strengths, corresponding to 750 and 800 MHz proton resonance frequencies, for solid-state NMR spectroscopy. McDermott et al.[1] clearly demonstrate that the resolution improvement at high field strengths will be essential to extend these studies to larger systems assembled in a membrane environment.

Solid-State NMR of Static Oriented Samples

When static spectra, those aquired without MAS, are measured in solids, the situation is much different. Orientation-dependent interactions, such as CSA and direct dipole–dipole coupling of nuclei one bond apart, such as between ^1H and ^{15}N, are then dominant, and multidimensional NMR spectra show the correlations between different anisotropic interactions. The appearance and usefulness of the spectrum depends on how the sample is oriented with respect to the magnetic field.

When the sample is highly oriented (Figure 1c), as a lipid bilayer might be, the spectrum consists of discrete resonances. The spectrum looks superficially like a MAS or solution-state NMR spectrum, but with the important distinction that the frequencies in each dimension depend on the molecular orientation with respect to the magnetic field. This property can be exploited to determine the direction of orientation of various parts of the molecule, and further analysis may reveal the overall structure of the molecule.

  1433-7851/01/4011-2046 $ 17.50+.50/0

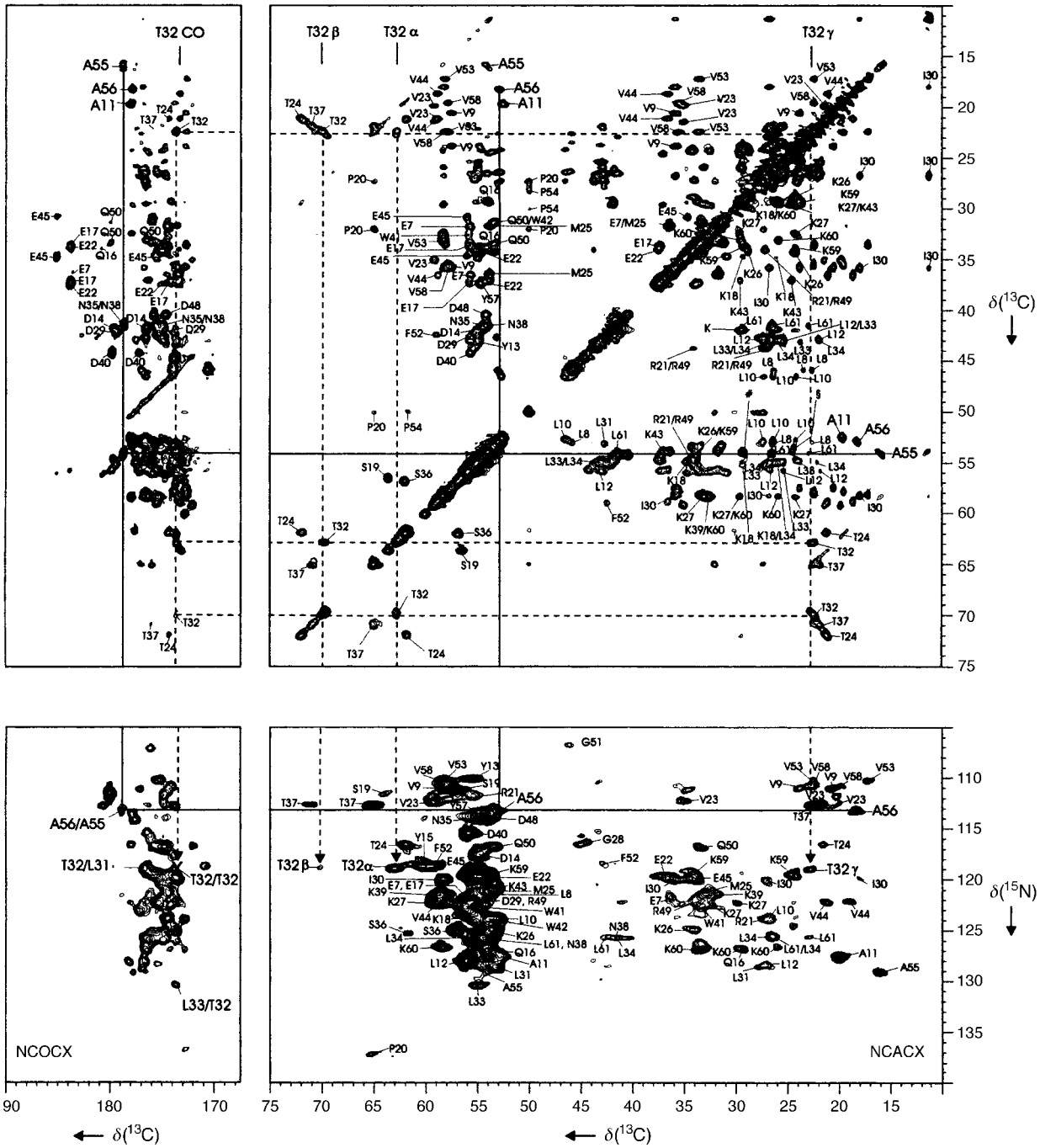

Figure 2. Two regions from a proton-driven spin-diffusion spectrum (PDSD) MAS solid-state spectrum of a uniformly ^{13}C,^{15}N-labeled sample of an SH3 domain. Above: The left panel contains cross peaks between aliphatic and carbonyl carbons, the right panel contains cross peaks between aliphatic carbons. Below: NCO (left) and NCA (right) regions of the NCOCX and NCACX spectrum, respectively. These Figures were kindly provided by H. Oschkinat.[2]

The PISEMA method[8] has been used extensively to study oriented systems. PISEMA is a two-dimensional NMR method for correlating the dipolar couplings between ^1H and ^{15}N in the first frequency domain ω_1 with the respective ^{15}N CSAs in ω_2. When applied to uniformly ^{15}N-enriched membrane proteins in oriented bilayers, PISEMA provides angular restraints of each amide site relative to the bilayer normal axis, which is normally mechanically aligned parallel to the magnetic field $\boldsymbol{B}_0$.[9] The traditional approach to analyzing PISEMA spectra requires careful resonance assignment of cross peaks in order to draw conclusions about the secondary structure. For larger proteins, there is an increasing problem of spectral congestion and overlap, which makes it more difficult to assign the complete spectrum. However, there is a promising new method to alleviate this difficulty, by extending PISEMA into a third dimension based on the amide ^1H CSA.[10]

Marassi and Opella[11] and the group of Cross[12] have recently recognized that secondary structure information may be determined simply by inspection of the 2D PISEMA

spectrum. Remarkably, this can reveal the presence of a helix and its tilt angle with respect to the bilayer and, after initial assignment, the angular displacement of one repetition unit relative to the next as well as the handedness of the helix. The dipolar coupling between ^{1}H and ^{15}N and the ^{15}N CSA can be described as tensors. While variations of the CSA may be significant and provide important structural and dynamic information, the two-dimensional signal $F(\omega_2,\omega_1)$ of the PISEMA experiment can be described to a good approximation using a fixed set of uniform values for the CSA tensor elements and their orientation within a peptide plane,[13] as given by Equation (1). In Equation (1), $\sigma_{11}=64$, $\sigma_{22}=77$, and $\sigma_{33}=217$ ppm and are the principal components of the ^{15}N CSA tensor; the dipole tensor and the σ_{33} component of the CSA tensor are at an angle of $\theta=17^\circ$ (see Figure 3b). The term $\nu_\parallel=-10.4$ kHz is the dipolar coupling found for an amide site parallel to $\boldsymbol{B}_0$, τ defines the tilt of the helix axis relative to $\boldsymbol{B}_0$ (and the bilayer normal), and ρ defines the rotational orientation of a specific site within the helix.

$$\begin{aligned} F(\omega_2,\omega_1) &= F(\mathrm{CSA}(\rho,\tau),\ \text{dipole}-\text{dipole coupling}(\rho,\tau)) \\ &= (\sigma_{11}(-0.828\cos\rho\sin\tau-0.558\sin\rho\sin\tau-0.047\cos\tau)^2 \\ &\quad+\sigma_{22}(0.554\cos\rho\sin\tau-0.803\sin\rho\sin\tau-0.220\cos\tau)^2 \\ &\quad+\sigma_{33}(-0.088\cos\rho\sin\tau+0.206\sin\rho\sin\tau \\ &\quad-0.975\cos\tau)^2),\nu_\parallel/2((-0.326\cos\rho\sin\tau+0.034\sin\rho\sin\tau \\ &\quad-0.946\cos\tau)^2-1)) \end{aligned} \tag{1}$$

The cyclic regularity of a helical structure displaces amide NH bonds in a regular manner along the helix. This leads to roughly elliptical patterns of peaks in 2D PISEMA spectra. Figure 3a shows a simulation of the PISEMA spectra as a function of the tilt τ of the helix with respect to the bilayer and the orientation ρ of specific amino acids. The position and shape of the observed ellipsoid in the PISEMA spectrum reflects the helix tilt angle τ. For an angle $\tau=15^\circ$, two sets of 18 peaks shifted to the downfield part of the ^{15}N spectrum are observed. The fine structure of each ellipsoid, 18 peaks for a regular α-helix, stems from the different amino acids within a helix. Their resonance positions reflect the rotational position of individual sites. The screw sense of the resonance pattern correlates with the helical handedness, as indicated by numbers for individual residues in Figure 3a. It is clear that from the spectral information, the handedness, the tilt, and the rotational displacement per residue (ideally 3.6 residues per turn) of the helices can be determined, and resonances can be assigned based on the position of their two-dimensional correlation peak in the PISEMA spectrum.

Solid-State NMR of Static, Orientionally Disordered Samples

Static (non-MAS) spectra of orientationally disordered solids (Figure 1b) are qualitatively very different from those of oriented samples. The distribution of molecular orientations with respect to the magnetic field leads to a distribution of frequencies, that is, the signal from each site is spread out into a so-called powder pattern. Undesirable spectral overlap is quite likely, unless the sample is labeled specifically at the sites of interest. In the multidimensional spectra of static samples, the signal is spread out in each dimension, typically

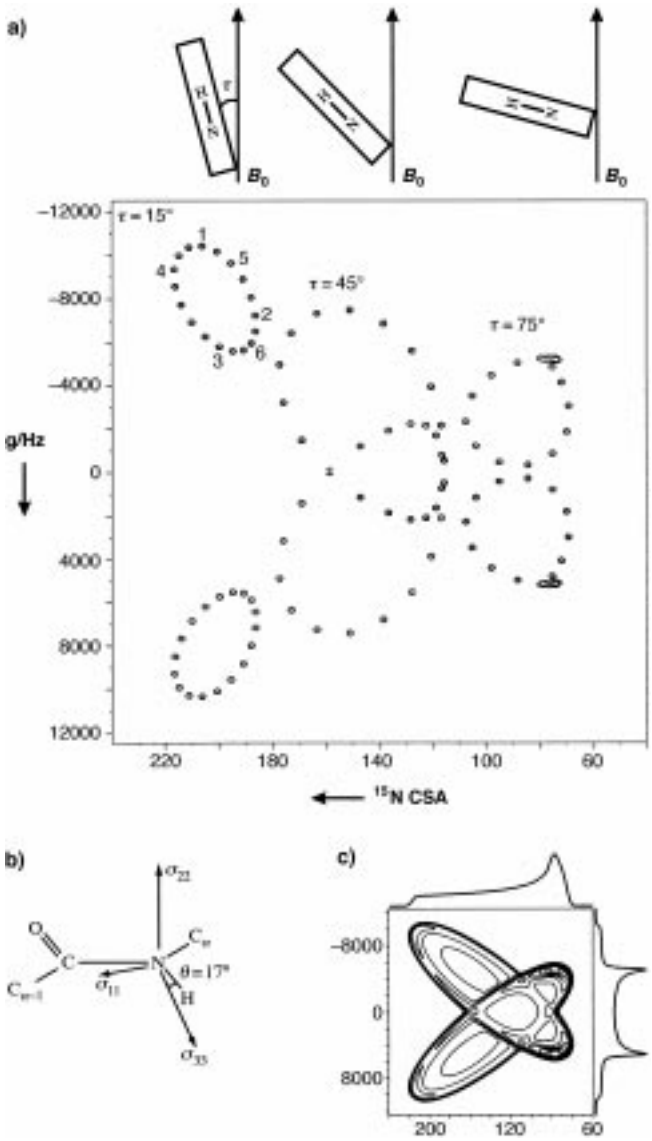

Figure 3. a) Simulation of the 2D PISEMA experiment for different orientations τ of the helix with respect to the bilayer normal. The simulations assume an ideal helix, standard bond angles for peptide planes, and standard values for the relative orientation of the dipole and chemical shift tensors. For each of the helical wheels, ρ (the rotation about the helix axis) was taken in 100° increments (namely, 3.6 residues per helix cycle) for 18 steps. Each peak within an ellipsoid represents a single amino acid residue in a regular helix oriented at an angle τ relative to the bilayer normal. The amino acid position along the helix is indicated for the tilt angle $\tau=15^\circ$. A right-handed helix will lead to a clockwise positioning of the resonance peaks of the amino acids in the helix (1–6 for $\tau=15^\circ$). b) Orientation of the ^{15}N CSA tensor elements in the peptide plane. c) Simulation of a dipolar–CSA correlation spectrum of an orientationally disordered sample. Projections along both dimensions reveal the CSA powder pattern (shown on the horizontal axis) and the dipolar Pake pattern (shown on the vertical axis). Parameters for the CSA and dipolar coupling were chosen as for Figure 3a, and an isotropic distribution within the powder was assumed.

forming a pattern of lobes and ridges that indicate the various anisotropic interactions and how they are correlated. A spectrum correlating ^{1}H–^{15}N dipole–dipole couplings with the respective ^{15}N CSAs in a static, orientationally disordered sample is shown in Figure 3c; it can be understood as a weighted summation over all helix orientations τ and ρ in

  1433-7851/01/4011-2048 $ 17.50+.50/0

Figure 3 a. These 2D powder patterns are usually analyzed by simulation and iterative fitting, and ultimately they are interpreted in terms of the relative orientations of dipolar and CSA tensors.

Another possibility is to correlate one CSA to another in the polypeptide chain. The group of Meier has used such an approach to determine the chain conformation of a silk protein. In their report, the chain conformation is revealed by examining correlations of ^{13}C CSAs between adjacent carbonyl sites in ^{13}C-labeled silk materials.[14] This was accomplished by double-quantum/single-quantum correlation spectroscopy that excites double-quantum coherence of adjacent carbonyl nuclei in the first evolution period of the 2D correlation experiment (DOQSY).[15] The orientation of the carbonyl CSA with respect to the C–O and C–N bonds is known from earlier work. With that, and other prior knowledge such as typical bond angles and distances, analysis of the DOQSY spectrum yields torsion angles of the protein backbone.

For a given pair of backbone torsion angles (ϕ,ψ), a distinctive 2D powder pattern is observed, as shown in Figure 4. Given an experimental powder pattern, one could solve for the torsion angles by iterative fitting, namely by adjusting ϕ and ψ as parameters of a simulation until it closely matches the measured spectrum. Van Beek et al.[14] performed a more sophisticated analysis that reconstituted the experimental 2D powder spectrum from simulated spectra weighted by the respective probability density $P(\phi,\psi)$.

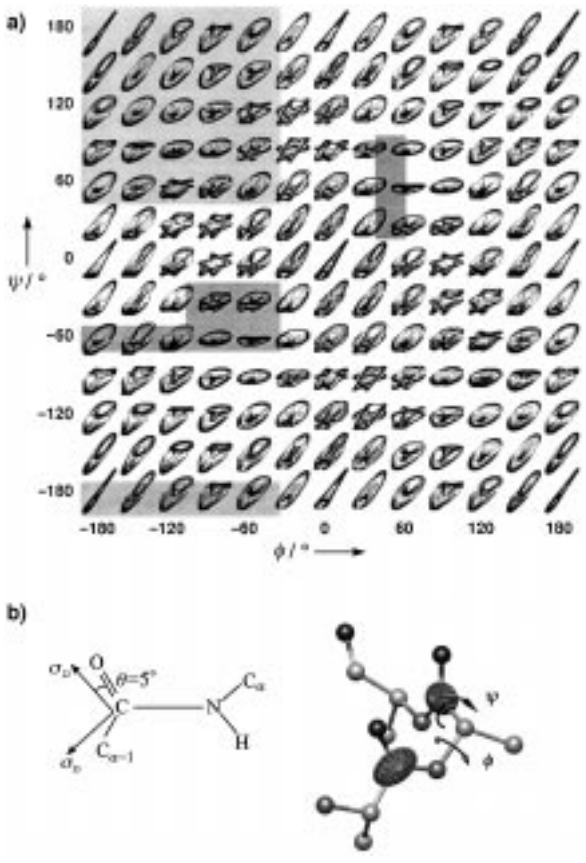

Figure 4. The (ϕ,ψ) dependence of DOQSY spectra in the two-spin approximation. a) Simulated DOQSY spectra as a function of (ϕ,ψ). Energetically favorable areas of the Ramachandran diagram are marked by a gray background. Each pattern represents a entire ^{13}C DOQSY spectrum, covering a chemical shift range of approximately $\delta = 490$ to 180 ppm in the vertical (double quantum) dimension, and $\delta = 245$ to 90 ppm in the horizontal (single quantum) dimension. b) Molecular orientation of a polypeptide and orientation of the ^{13}C CSA tensor elements in the peptide plane. The following CSA values have been assumed: $\sigma_{33} = 244.8$, $\sigma_{22} = 194.7$, and $\sigma_{11} = 91.6$ ppm, and $\theta = 5°$. The Figure is reproduced, with small alterations, with permission from *Nature*.

Symmetry relations are evident in Figure 4. The patterns are identical for (ϕ,ψ) and ($-\phi$, $-\psi$), and one consequence is that DOQSY itself cannot distinguish between left- and right-handed helices. In addition, spectra arising from torsion angle pairs (ϕ,ψ) and (ψ,ϕ) are similar. As van Beek et al.[14] mention, the two conformations have similar CSA–CSA correlations, which leads to a similarity in the overall outline of the DOQSY pattern. However, there is a difference in the dipolar–CSA correlation, which influences the intensity distribution over the pattern. This breaks the symmetry and allows distinction between these torsion angle pairs.

The DOQSY experiment yields particularly unambiguous results when the protein is isotopically labeled at specific sites. For the silk protein study, this was achieved by feeding ^{13}C carbonyl-labeled alanine to silkworms, with the expectation that alanine–alanine pairs with ^{13}C labeling in adjacent sites would appear predominantly in polyalanine domains. The application of the DOQSY technique to other proteins will require labeling schemes which are similarly well chosen for the particular system at hand.

The mechanical properties of silk depend on the state of polyalanine domains, which form small crystallites embedded within the fiber.[16] In natural silk fibers, the DOQSY spectrum indicates that the polyalanine domains exist in a β-sheet arrangement. In the same study,[14] a "silk" solid film was prepared from fluid withdrawn directly from the silk gland, and the DOQSY spectrum revealed that the polyalanine domains were in the α-helical form. These experimental data suggest that the structure of the silk protein depends sensitively on the method of its preparation.

The few examples in this article demonstrate some of the recent excitement in solid-state NMR: It seems possible to assign uniformly labeled proteins in their solid state. Tensor correlations in oriented and in orientationally disordered samples allow the determination of secondary structure elements with high precision. In addition, the tensor-correlation experiments[15] have considerable impact on new experiments in liquid NMR spectroscopy,[17–19] so that two fields of NMR, distinct in the past, are now merging together.

[1] A. McDermott, T. Polenova, A. Bockmann, K. W. Zilm, E. K. Paulsen, R. W. Martin, G. T. Montelione, *J. Biomol. NMR* **2000**, *16*, 209–219.
[2] J. Pauli, M. Baldus, B. van Rossum, H. de Groot, H. Oschkinat, *ChemBioChem*, **2001**, *2*, 272–281.
[3] J. Pauli, B. van Rossum, H. Förster, H. J. M. de Groot, H. Oschkinat, *J. Magn. Reson.* **2000**, *143*, 411–416.
[4] R. G. Griffin, *Nat. Struct. Biol.* **1998**, *5*, 508–512 (Supplement), and references therein.
[5] M. Baldus, A. T. Petkova, J. Herzfeld, R. G. Griffin, *Mol. Phys.* **1998**, *95*, 1197–1207.
[6] K. Nomura, K. Takegoshi, T. Terao, K. Uchida, M. Kainosho, *J. Biomol. NMR* **2000**, *17*, 111–123; S. Dusold, A. Sebald, *Annu. Rep. NMR Spectrosc.* **2000**, *41*, 185–264.

[7] K. Schmidt-Rohr, *J. Am. Chem. Soc.* **1996**, *118*, 7601 – 7603; X. Feng, Y. K. Lee, D. Sandström, M. Edén, H. Maisel, A. Sebald, M. H. Levitt, *Chem. Phys. Lett*. **1996**, *257*, 314 – 320; X. Feng, P. J. E. Verdegem, Y. K. Lee, D. Sandström, M. Edén, P. Bovee-Geurts, J. W. de Grip, J. Lugtenburg, H. J. M. de Groot, M. H. Levitt, *J. Am. Chem. Soc.* **1997**, *119*, 6853 – 6857; P. R. Costa, J. D. Gross, M. Hong, R. G. Griffin, *Chem. Phys. Lett.* **1997**, *280*, 95 – 103; M. Hohwy, C. P. Jaroniec, B. Reif, C. M. Rienstra, R. G. Griffin, *J. Am. Chem. Soc.* **2000**, *122*, 3219 – 3219.
[8] H. Wu, A. Ramamoorthy, S. J. Opella, *J. Magn. Reson. A* **1994**, *109*, 270 – 272.
[9] S. J. Opella, Y. Kim, P. McDonnell, *Methods Enzymol.* **1994**, *239*, 536 – 560.
[10] F. M. Marassi, C. Ma, J. J. Gesell, S. J. Opella, *J. Magn. Reson.* **2000**, *144*, 156 – 161.
[11] F. M. Marassi, S. J. Opella, *J. Magn. Reson.* **2000**, *144*, 150 – 155.
[12] J. Wang, J. Denny, C. Tian, S. Kim, Y. Mo, F. Kovacs, Z. Song, K. Nishimura, Z. Gan, R. Fu, J. R. Quine, T. A. Cross, *J. Magn. Reson.* **2000**, *144*, 162 – 167.
[13] G. S. Harbison, L. W. Jelinski, R. E. Stark, D. A. Torchia, J. Herzfeld, R. G. Griffin, *J. Magn. Reson.* **1984**, *60*, 79 – 82; C. J. Hartzell, M. Whitfield, T. G. Oas, G. P. Drobny, *J. Am. Chem. Soc.* **1987**, *109*, 5862 – 5866; Q. Teng, T. A. Cross, *J. Magn. Reson.* **1989**, *85*, 439 – 447.
[14] J. D. van Beek, L. Beaulieu, H. Schäfer, M Demura, T. Asakura, B. H. Meier, *Nature* **2000**, *405*, 1077 – 1079.
[15] M. Linder, A. Hoehner, R. R. Ernst, *J. Chem. Phys.* **1980**, *73*, 4959 – 4970; P. M. Henrichs, M. Linder, *J. Magn. Reson.* **1984**, *58*, 458 – 461; K. Schmidt-Rohr, *Macromolecules* **1996**, *29*, 3975 – 3981.
[16] Z. Yang, P. T. Grubb, L. W. Jelinski, *Macromolecules* **1997**, 30, 8254 – 8261.
[17] K. Pervushin, R. Riek, G. Wider, K. Wüthrich, *Proc. Natl. Acad. Sci USA* **1997**, *94*, 12366 – 12371.
[18] B. Reif, M. Hennig, C. Griesinger, *Science* **1997**, *276*, 1230 – 1233; D. Yang, L. E. Kay, *J. Am. Chem. Soc.* **1998**, *120*, 9880 – 9887; I. C. Felli, C. Richter, C. Griesinger, H. Schwalbe, *J. Am. Chem. Soc.* **1999**, *121*, 1956 – 1957; P. Pelupessy, E. Chiarparin, R. Ghose, G. Bodenhausen, *J. Biomol. NMR* **1999**, *13*, 375 – 380.
[19] J. Boyd, C. Redfield, *J. Am. Chem. Soc.* **1999**, *121*, 7441 – 7442; J. Boyd, C. Redfield, *J. Am. Chem. Soc.* **1999**, *121*, 9692 – 9693.

  1433-7851/01/4011-2050 $ 17.50+.50/0